ISOPHOT IN-FLIGHT CALIBRATION STRATEGIES

U. Klaas[1], P. Ábrahám[1,2], J. A. Acosta-Pulido[3], P. Héraudeau[1], C. Kiss[1,2], R. J. Laureijs[4], D. Lemke[1], P. J. Richards[5], B. Schulz[2] and M. Stickel[1]

[1]Max-Planck-Institut für Astronomie, Heidelberg, Germany
[2]Konkoly Observatory of the Hungarian Academy of Sciences, Budapest, Hungary
[3]Instituto de Astrofísica de Canarias, Tenerife, Spain
[4]ISO Data Centre, European Space Agency, Villafranca del Castillo, P.O. Box 50727, 28080 Madrid, Spain
[5]CLRC, Rutherford Appleton Laboratory, Chilton, Didcot, United Kingdom

ABSTRACT

ISOPHOT, the imaging spectro-photo-polarimeter on board ISO, supported performance of aperture and mapping photometry, low-resolution spectroscopy and polarimetry, both in staring and chopped mode. In addition, the 170 μm ISOPHOT Serendipity Survey was performed while slewing from one target to the next. Its calibration had to be connected to the pointed and raster observations. One initial aspect of the calibration program was the finding of optimal observation strategies (chopping, mini-maps, absolute photometry) depending on source type. FIR detection limits were determined facing the in-orbit radiation environment and the inhomogeneous sky background. ISOPHOT's large wavelength range from 2.5 to 240 μm, covered by 25 filters in combination with subsets of 17 different apertures or array/pixel sizes, combined with a large dynamic range set the frame of requirements on calibration measurements and standards. Based on the pre-flight characterisation a list of requirements was worked out as a guide for the calibration planning. An important item in the absolute photometric calibration was the reference to celestial standards via a transfer calibration using the internal reference sources. This became particularly demanding when one of the internal reference sources changed its radiation properties in the early routine phase. We give an overview of standard sources, calibration strategies for each main observational mode and the accuracies achieved so far. With the end of the ISO Post Operations Phase the scientific validation status of most of the ISOPHOT observing modes has been established.

Key words: Instrumentation: detectors – Instrumentation: photometers – Space vehicles: instruments – Infrared: general

1. INTRODUCTION

The calibration of ISOPHOT (Lemke et al. 1996) comprised the calibration of 4 sub-instruments (Table 1).
Specific calibration aspects from the instrument design and operation were therefore:

- the large wavelength range (2.5 – 240 μm);
- the large dynamic range by the aperture areas (5 – 180$''$ diameter);
- the large flux range (4 – 5 decades);
- the variety of sampling of apertures by rasters;
- the optional use of the chopper for differential measurements and resolution enhancement;
- the operation of low background detectors in the cosmic ray environment;
- the various detector types – the stressed Ge:Ga detectors were operated for the first time in space;
- the signal transients of the photoconductive detectors.

Table 1. ISOPHOT sub-instruments.

sub-instrument	λ range [μm]	designation
aperture photometer	3 – 100	PHT-P
array cameras	60 – 200	PHT-C
low-resolution spectrometer	2.5 – 12	PHT-S
two polarimetric channels	25, 170	PHT-P & C polarizers

Since it would have been time consuming to cover the whole parameter space of instrument set-ups by measurements, first some key instrument configurations had to be defined. The design of the instrument allowed polarimetry with all 25 filters and the full set of apertures. After an extensive test campaign, this mode was restricted to the most stable detectors in combination with the most sensitive filters.

2. AOT DESIGN AND OPERATIONS

Some calibration strategies were included in the design of the observational modes (AOTs) in order to minimise certain instrumental effects. The most important ones are listed in Table 2.

Some calibration measurements were set up by the way of operating the instrument. The most important ones are listed in Table 3. For a detailed description of the in-flight curing and re-curing procedures, see Wilke et al. (2003).

3. IN-ORBIT CALIBRATION REQUIREMENTS

The in-orbit calibration requirements were established pre-flight as an outcome of the instrument ground calibration (Lemke et al. 2003a). They were compiled in a document (IOCRD) and proved to be a complete check list in-flight. There were 5 major subjects, with a total of 63 requirements (Table 4).

Proceedings of the Conference "The Calibration Legacy of the ISO Mission", VilSpa, Spain, February 2001
ESA SP-481, 2003, eds. L. Metcalfe, A. Salama, S. B. Peschke & M. F. Kessler

Table 2. Calibration strategies included in AOT design.

instrumental effect		strategy
cope with detector responsivity variations	⇒	inclusion of ≥ 1 FCS measurement per detector (except PHT-S, AOT PHT40)
minimise signal transients	⇒	order filter sequence by increasing flux (faster settling times)
	⇒	order aperture sequence by increasing flux
	⇒	adjust FCS measurement to expected total sky flux & use same configuration
	⇒	use sufficiently long measurement times, force lower limits
	⇒	redesign absolute photometry from chopped to long lasting staring measurements
correct for offsets	⇒	include dark signal & bypassing skylight assessment in absolute mode
detect memory effects	⇒	dark preceding PHT-S sky measurement
avoid detector switch-on effects	⇒	detectors remain on during sparse map execution

One advantage of the comprehensive pre-flight tests was that the optimum detector bias voltages and operational temperatures had been well defined and needed no change in-orbit.

The ISOPHOT Instrument Dedicated Team (PIDT) designed and implemented > 2800 calibration measurements. On top of those numerous scientific observations are useful to extend the calibration data base.

4. SCIENCE WINDOW EXTENSION TESTS

Early in the Performance Verification Phase it was discovered that a window somewhat longer than specified might be available for scientific observations. The PIDT tested this for ISOPHOT under restricted conditions:

1) 7 revolutions during the Performance Verification (PV) Phase (in between revolutions 37 and 61) were allocated. This period covered only 0.8 months of the mission and did not take into account the annual variation of the environment along ISO's orbit with regard to the Earth's radiation belts.
2) No stable pointing was guaranteed, because ISO was switched to the Perigee Passage Mode.
3) No OLP processing was possible, because observations were outside the nominal science window at that time. The assessment of data quality had to be done with the help of QLA (Quick-look Analysis) strip maps.

Table 3. Calibration strategies covered by (daily) operations.

instrumental effect		strategy
establish reproducible calibration after passage of radiation belts	⇒	effective curing procedure during activation window before opening of science window
monitor stability of FCS	⇒	responsivity check after curing
	⇒	monitoring measurements of faint & bright standards
stabilise detector responsivity	⇒	re-curing of FIR detectors including noise reduction in handover window at apogee
monitor responsivity behaviour of PHT-S (no FCS)	⇒	responsivity checks in activation & deactivation

Table 4. Main subjects of ISOPHOT in-orbit calibration and their coverage by requirements and measurements. Measurements during the Satellite Commissioning Phase (SCP) were partly manual procedures, and may have non-standard products in the ISO archive.

	subject	no. reqs.	no. meas.
1	Electronics & Detectors	17	287 + SCP
2	Photometric Calibration FCS, flat-fields	18	2111
3	Spectral Calibration	6	6
4	Footprints & Straylight	14	238 + SCP
5	Various: Instrumental Polarisation, Cross calibration, Serendipity Mode calibration, local IR backgrounds	8	166

The period up to 1.5 hours after the end of the nominal window was explored by staring with one detector on a calibration star (as long as not restriction 2 above applied). The test results as summarised in Table 5 supported the extension of the science window by 45 min. However, during the mission occasionaly data quality degraded in the last hour. The experience with the full mission knowledge is that responsivities and dark signals show a higher scatter towards the end of the science window (Wilke et al. 2003, del Burgo et al. 2003). One impact is that measurements of faint sources are less sensitive and accurate (see e.g. Figure 3). Ideally these measurements should have been always scheduled in good parts of the science window, which would have meant an extra requirement on the mission planning system to recognise such observations.

Table 5. Outcome of science window extension tests.

rev.	detector	result
37	P2	extension possible by 1 h
41	P1	high glitch rate after 0.5 h
45	C200	extension possible by 1 h
49	C100	high glitch rate after 0.0 h
53	P3	extension possible by 1 h
57	S	extension possible by 0.75 h
61	P2	extension possible by 1.5 h

5. CHANGE OF FCS RADIATION CHARACTERISTICS

An important item in the absolute photometric calibration was the reference to celestial standards via a transfer calibration using the internal reference sources, the FCS (Fine Calibration Sources). ISOPHOT had 2 FCS units with a total of 4 Thermal Radiation Sources (TRS), two each for short and long wavelength detectors. The FCS1/TRS2 was the main reference source for the P3, C100 and C200 detectors. On revolution 94 an anomalous event occurred which changed the radiation characteristics of this source. It was very likely a flake-off of the NiCr coating from the surface of the little diamond heater. This was noticed as “failed curing” in activation through the signals of the post curing responsivity checks being above the threshold. The signal increase with a factor of about 2 remained on subsequent revolutions. Comparison of the FCS1/TRS2 signals with FCS2/TRS2 and celestial standard star signals before and after revolution 94 showed relative constancy of the latter two, but a change in the FCS1/TRS2 signals. With this event the Performance Verification Phase data base for FCS calibration became invalid for the FIR detectors.
The procedure after the event was:

- keep the FCS1/TRS2 as the main calibrator for the FIR detectors, a switch to FCS2/TRS2 would have had a major impact on the AOT logic;
- intensify the re-calibration and add calibration measurements of the redundant source FCS2/TRS2;
- monitor both sources against bright and faint celestial standards.

There was no further change of the FCS1/TRS2 emission during the mission. Hence a two period time dependent FCS calibration is performed in data reduction. The quality is somewhat lower for observations before revolution 94, on the other hand this period comprises a minority of the total number of observations.

6. FAINT SOURCE DETECTION LIMITS

A major undertaking was the establishment of the optimum observation mode for faint sources. Initial tests during the Performance Verification Phase suggested a nominal performance: chopped observations clearly detected the IRAS Deep Survey source 17504+6722 (Hacking & Houck 1987) with f_{60} = 110 mJy and f_{100} = 330 mJy. We designed a program on faint stars to establish systematically detection limits of the following ISOPHOT modes which had been offered for faint source observations:

a) staring sequences off–on–off–on... (in the beginning executed via a sparse map, which was later replaced by telescope nodding);
b) chopping (triangular mode for P1, P2, P3, C100, rectangular mode for C200);
c) staring raster mini-map (for PHT-C only);
d) chopped high resolution raster map (for PHT-C only).

Five faint stars were observed in these four different modes. The most reliable and accurate observing modes turned out to be nodding for PHT–P and the staring mini-map for PHT–C. Following a workshop in February 1997 these modes were recommended to the observers (Laureijs & Levine 1997). It was important to test the real observing modes in-flight on a sufficient number of sources to come to these clear conclusions.

The FIR detector sensitivities were limited by sky confusion noise, a concrete example is shown in Figure 1. Kiss et al. (2001) evaluated 175 ISOPHOT maps at 90, 100, 170 and 200 μm and determined instrumental and sky confusion noise. The C200 measurements were verified to be sky confusion noise limited for the whole surface brightness range.

7. CALIBRATION SOURCES FOR ISOPHOT

For the photometric and spectrophotometric calibration in the NIR and MIR stars were used as celestial standards. Stellar models as flux references were provided by M. Cohen and P. Hammersley (Cohen 2003, Hammersley 2003).
For the photometric calibration in the FIR three different types of calibrators were used:

a) the planets Uranus and Neptune at the bright flux end (150 – 1000 Jy) (Burgdorf & Orton 2003);
b) the brightest stars at the faint flux end (0.1 – 20 Jy) (extensions of stellar models to the FIR; see Cohen 2003);
c) asteroids for a wide intermediate flux range (1.5 – 150 Jy). Improved flux predictions became available by the application of thermophysical models (Müller & Lagerros 2003).

The availability of a large number of well defined calibration sources was important in order to establish a good coverage of the ISOPHOT detector flux ranges and to cope with nonlinearity or transient effects, see Schulz (2003) and Acosta-Pulido & Ábrahám (2003).

8. CALIBRATION STATUS FOR LEGACY ARCHIVE

A measure for the success and completeness of a calibration strategy of a versatile space instrument like ISOPHOT is the set of finally achieved calibration accuracies of the data products in the ISO Legacy Archive. ISOPHOT offered 11 types

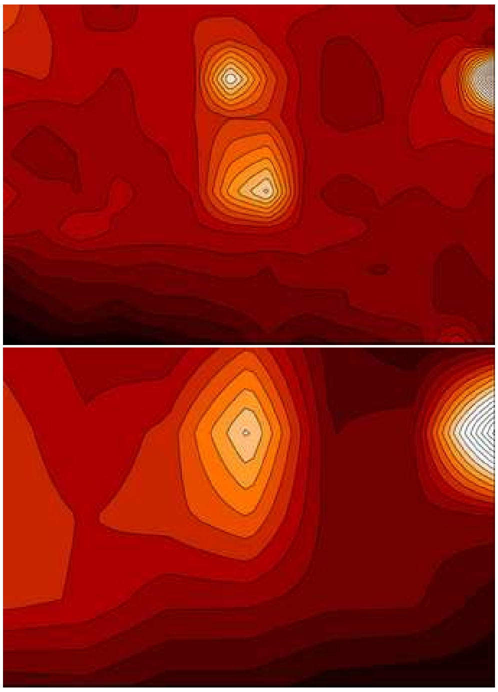

Figure 1. ISOPHOT faint source detection strategy tests on the star HR 6132 (f_{90} = 288 mJy, f_{170} = 79 mJy). Upper image is at 90 µm, lower image at 170 µm. The images show the results of staring raster maps around the source which is located in the centre. ISSA maps do not show any high sky background in its immediate environment. In the 90 µm map the star can be clearly recognised at the centre. There are two more discrete point sources in the field, one is located quite close to the star. In the 170 µm map, due to lower resolution and the other source being relatively brighter than the star, the double source is smeared out to an elongated structure with the peak being shifted towards the brighter neighbouring source. Hence, the 170 µm observation of HR 6132 is sky confusion noise limited.

of observation with in total 28 submodes plus the ISOPHOT Serendipity Survey. In the following we will consider the main modes in some detail and conclude with a status overview of all observing modes.

In order to achieve these results, the following steps were important:

1) During the mission repeated reviews of the completeness of the calibration were held. Comprehensive statistics on the selected instrument set-ups helped to cover a large fraction of observations.
2) A step-by-step characterisation of instrumental effects starting with the observing modes closest to calibration procedures.
3) Calibration analysis was exclusively done by using the PHT Interactive Analysis (PIA, Gabriel 2003), partly using semi-automatic procedures in case of big data bases. New calibration items were usually checked out in PIA before their implementation into the pipeline (OLP) system. For this last step the implementation requirements had to be verified for robustness inside a fully automatic system.
4) A systematic check-out of a representative set of OLP data products in scientific validation (Richards et al. 2003).

8.1. Staring Mode Photometry

This type of photometry was the basic ISOPHOT observing mode. The photometric calibration against celestial standards was performed in staring mode (see Schulz 2003). Most instrumental effects were therefore characterised from this mode.

The achieved calibration accuracies for the simple on-off photometry are summarised in Table 6, an example over a wide wavelength and flux range is shown in Figure 2. As can be seen from this example, the accuracy of the simple on-off mode is limited for faint sources on a bright background. Then more sophisticated modes like nodding or mini-map photometry were required.

Table 6. Accuracies for staring mode on-off photometry. Photometry of fainter sources required more sophisticated modes, see e.g. Table 7.

detector	flux range [Jy]	absolute accuracy [%]	reproduc. 1 σ of 20 samples [%]	multi-filter accuracy [%]
P1	30 – 6000	<10	5	<20
P2	10 – 200	<10	2	5
P3	5 – 25	10	7	<10
C100	5 – 25	15	$\geq$3	<25
C200	2 – 900	10	10	<20

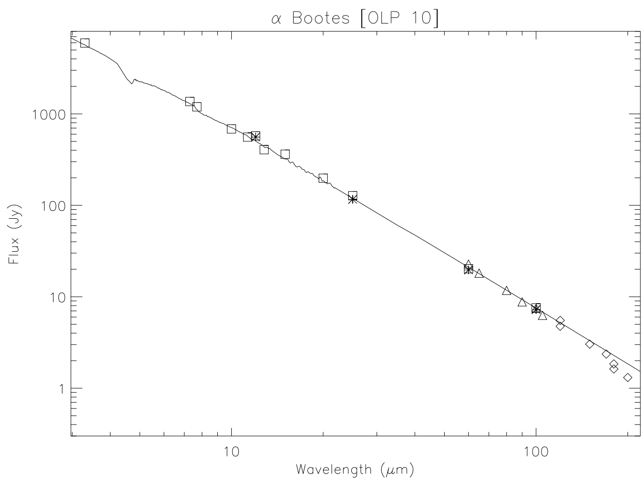

Figure 2. ISOPHOT multi-filter on-off staring mode photometry of α Bootes. For this OLP validation case all 25 ISOPHOT filters were used. The example demonstrates the quality of the ISOPHOT calibration over nearly 4 decades in flux. In the wavelength range 100 – 200 µm, the background amounts to 1 – 5 times the source flux. Squares, triangles and diamonds label the ISOPHOT photometry with PHT–P, C100 and C200, and asterisks the IRAS photometry.

8.2. PHT–C Mini-map Photometry

This mode proved to be the most sensitive and accurate observation strategy for the FIR arrays. It has several advantages, namely:

- pixel redundancy, the essential parts of the map are covered by each pixel;
- the source is centred on each pixel;
- the measurement mode is closest to the FCS calibration strategy of the arrays.

The achieved calibration accuracies are listed in Table 7. This mode was used to establish the reproducibility of the calibration for the C-arrays (Figure 3).

Table 7. Accuracies for PHT–C mini-map photometry.

detector	flux range [Jy]	abs. accuracy [%]	reproducibility [%]
C100	> 0.5	5	≥ 3
	0.05 – 0.5	<25	20
C200	0.25 – 1000	<20	10

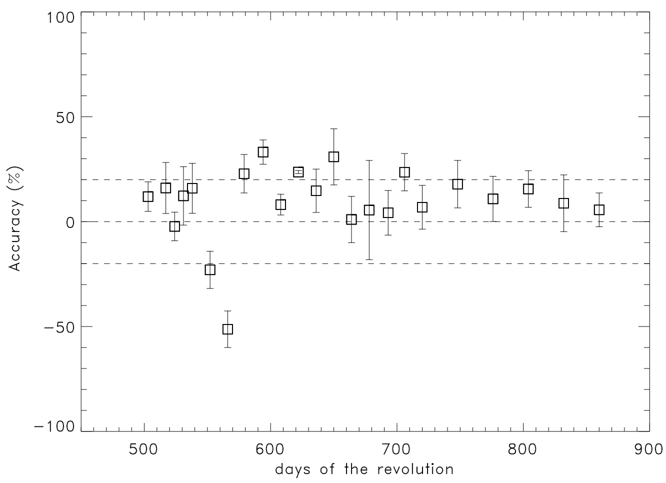

Figure 3. Monitoring of the faint calibration star HR 7310 (f_{100} = 200 mJy) using the mini-map mode. The absolute accuracy determined as the deviation from the model flux is displayed versus the day of the revolution. The error bars give the flux reproducibility by all 9 pixels, since the source is centred on each of them along the raster. The two outliers between revolutions 550 and 570 correspond to observations close to the end of the science window.

8.3. Chopped Photometry

This mode required the characterisation of additional instrumental effects due to its different design:

- Because of the in general small number of ramps per chopper plateau a chopped pattern is constructed from the various chopper cycles in order to cope with glitches and derive a robust signal difference.
- The relatively short dwell times on the source and the reference position do not allow transients to settle. Empirical signal loss corrections had to be established relative to stabilised staring measurements.
- The signal loss correction also applies to the FCS measurements, which were performed in chopped mode, too. The transient behaviour is however different from sky measurements and the relatively short exposure time of the FCS measurement does not allow to establish a chopped pattern which is as robust as that for the sky measurement. In addition absolute signal levels instead of differential ones are needed for the determination of the actual responsivity. Therefore, the use of the mission averaged responsivities (so-called default responsivities) instead of the actual responsivity was tested. For the P2 detector this approach gives more accurate results.

A detailed overview of this mode is given by Ábrahám et al. (2003). Accuracies achieved with OLP version 10.0 are given in Table 8. For the FIR detectors general accuracy numbers are difficult to derive for sources fainter than 1 Jy, since the relatively bright sky background and the small number of reference positions make an estimate of the cirrus confusion noise necessary (cf. Section 6).

Table 8. Accuracies for chopped photometry achieved with the Legacy Pipeline, OLP 10. For C200 no reproducibility could be derived due to cirrus confusion of the reference target.

detector	flux range [Jy]	abs. accuracy [%]	reproducibility $1\,\sigma$ of 6 samples [%]
P1	0.06 – 10	<30	<15
P2	0.2 – 20	<30	<10
P3	$\geq$1	<30	<10
C100	$\geq$1	<30	<15
C200	$\geq$2	<40	–

8.4. Extended Source Photometry

Due to the lack of suitable extended source calibrators the absolute photometric calibration of ISOPHOT is solely based on point sources. In order to convert to surface brightness the wavelength dependent effective solid angles had to be determined. The backbone calibrations were high quality forward and backward linear scans across key apertures in key filters. Gaps in the parameter space had to be filled by modelling. In addition it was checked that the extended wings of the beams are not contaminated by straylight (Lemke et al. 2003b). This was done for the near-field ($\sim$1°) of very bright point sources. Potential straylight from the three most relevant infrared emitting bodies, Moon, Sun and Earth, was measured near the avoidance angles (24°, 60° and 87°, when the Earth illuminated the inside of the sunshade).

A useful reference for the assessment of surface brightness accuracies is the COBE/DIRBE data base, however, for a proper comparison corrections for the different beam sizes, background structures and source colours have to be done (Héraudeau et al. 2003).

A simple consistency check without applying any of these corrections is shown in Table 9.

Table 9. Accuracies for extended source photometry achieved with the Legacy Pipeline, OLP 10. The large flux range is covered by larger maps, the small flux range by multi-filter background measurements allowing assessment of relative filter-to-filter accuracies. The numbers are derived from a simple consistency check with the DIRBE photometry.

detector	flux range [MJy sr^{-1}]	abs. accuracy [%]	rel. accuracy [%]
C100	5 – 15	<25	20
	5 – 400	<25	–
C200	4 – 10	<25	20
	3 – 600	<25	–

Maps generated using the FCS illumination to calibrate the pixels relative to each other showed residual flat-field patterns, in particular those with no pixel overlap. Flat-fielding accuracies of large maps have been improved by a statistical method (Table 10). Using the surface brightness distribution of the map itself the 10%ile surface brightness values (representing the sky background level) for each pixel are derived and the correction factors are determined as the ratios to the average 10%ile for all pixels. An example is given in Richards et al. (2003).

Table 10. Flat-field accuracies achieved with the Legacy Pipeline, OLP 10, for large maps, by applying a statistical flat-field derived from the 10%ile surface brightness values in addition to the standard photometric calibration with the FCS.

detector	flat-field accuracy no pixel overlap [%]	with pixel overlap [%]
C100	4 – 10	3 – 6
C200	2 – 6	2 – 4

The most complex observing mode of ISOPHOT, high resolution mapping in chopped mode (AOT PHT32) benefited in data quality from algorithmic developments in other fields. By applying a robust averaging method on pairs of read-outs of the same chopper plateau, developed for pointed chopped observations, and the statistical flat-field method, developed for staring raster maps, the mode could finally be partially validated with regard to surface brightness calibration and flat-field quality. The drastic reduction in the number of glitches allows for higher contrasts and better intercomparability of maps in different filters (Figure 4). A more sophisticated, but purely interactive method, correcting also for the signal transients to achieve accurate photometry for bright point sources in the map, has been developed by Tuffs (2002).

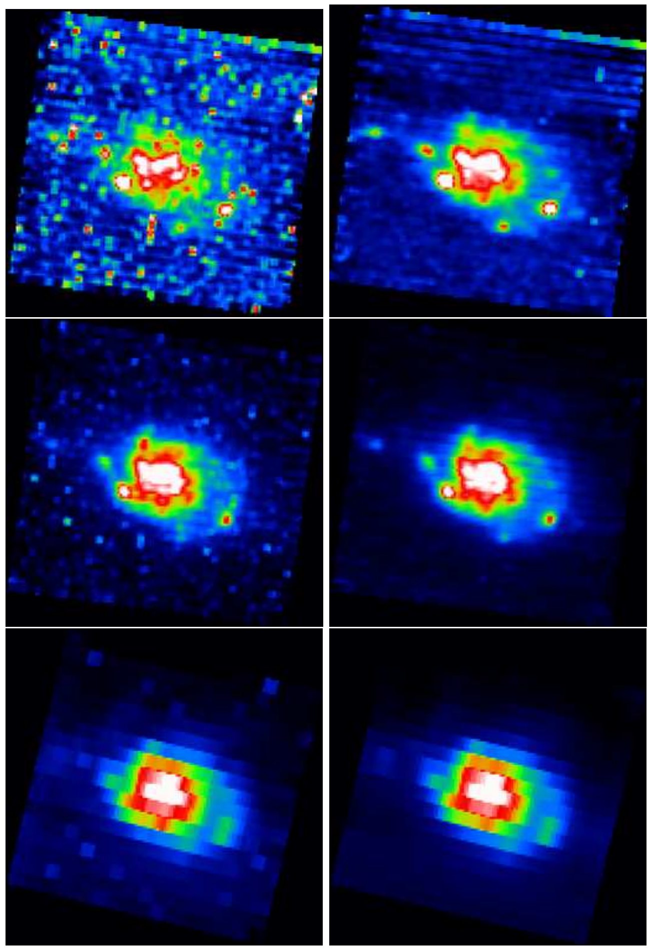

Figure 4. Improvement of the deglitching and flat-field accuracy of chopped raster maps obtained with AOT PHT32. 60 μm (top), 100 μm (middle) and 170 μm (bottom) images of M101 without (left) and with (right) deglitching and the statistical flat-field method.

8.5. PHT–S Spectrophotometric Calibration

The spectrophotometric calibration of ISOPHOT-S was different from the other observing modes as it was not based on a transfer calibration with the internal FCSs. This was possible, because PHT-S did not show any systematic responsivity changes along the revolution and with mission time. Therefore, measurements of calibration stars taken over the whole mission could be used to establish a calibration scheme, provided they were obtained with the same fixed measurement sequence as the unknown source.

For staring mode observations the dynamic spectral response calibration is applied. For each target the spectral response function is individually composed from calibration data cubes making use of the fact that for each pixel a measurement of a celestial standard of similar brightness shows the same temporal transient behaviour as for the source measurement. Therefore, for each period in time, as defined by the selected length of an integration ramp, the spectral response function is adjusted to give the appropriate present signal-to-flux conversion. The only limitation is that this method applies to a certain temperature range of the PHT–S detectors. During the Performance Verification Phase with mainly one-instrument operation per revolution, and occasionally during the Routine Phase, the temperature range requirement was not fulfilled and spectra have a degraded quality.

For chopped observations an average spectral response function was constructed from chopped observations of standard stars. A first order correction is added to this which is dependent on the flux step. The only limitation of this method is the flux range covered by standards, but it is fairly complete.

Both calibration methods contain an intrinsic transient correction established from measurements and give very accurate results (Table 11 and Figure 5). For extended sources similar accuracies are achieved down to the zodiacal light level, provided the measurement time is $>$1024 s. More details are given by Acosta-Pulido & Ábrahám (2003).

Table 11. Spectrophotometric accuracies for staring and chopped observations with PHT–S.

det.	mode	flux range [Jy]	abs. accuracy [%]	rel. accuracy [%]
SS	on-off	1 – 6000	<10	<15
	chopped	0.5 – 500	<10	10
SL	on-off	0.3 – 1500	<10	<15
	chopped	0.2 – 200	<10	10

8.6. POLARIMETRY

The key parameter for the achievable polarimetric accuracy is the source-to-background contrast. In order to maximise it for the 2×2 C200 array the source was centred on each pixel by executing a small raster map, which provided four-fold redundancy. For derivation of uncertainties the reproducibility is essential, a loop through several polariser cycles with sufficient stabilisation times per polariser setting was performed, rather than performing one single cycle with long integration times per polariser. An overview of the achieved 1 σ polarisation errors is given in Klaas et al. (1999).

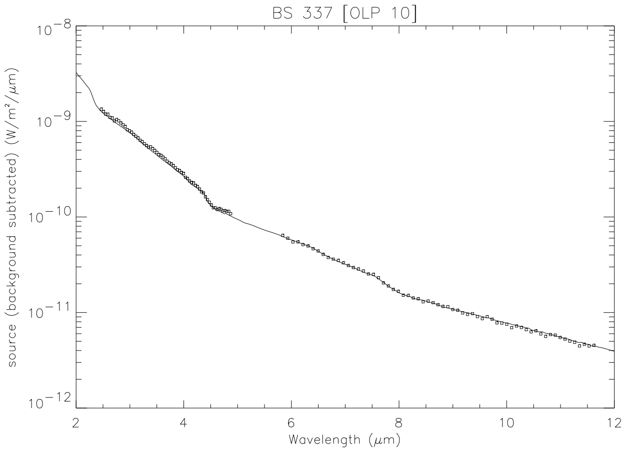

Figure 5. ISOPHOT on-off staring mode spectrophotometry of the point source BS 337. This is a consistency check of the performance of the dynamic spectral response calibration on a calibration star. The calibrated ISOPHOT–S spectrum (squares) is overlaid on the stellar model by M. Cohen (solid line) and shows a perfect agreement.

Instrumental polarisation was derived from observations of unpolarised sources or sky background fields. The values are given in Klaas et al. (1999) for 25 μm and Laureijs & Klaas (1999) for 170 μm.

8.7. CALIBRATION OF SERENDIPITY SURVEY POINT SOURCES

The derivation of point source fluxes from the ISOPHOT 170 μm Serendipity Survey consists of the following steps which are unique to that mode:

1) Subtraction of a large scale background from the surface brightness calibrated data stream.
2) Removal of one-sample-wide cosmic ray hits.
3) Phase-shifted averaging of pixel data streams.
4) Identification of source candidates as peaks $>3\,\sigma$ of the local noise.
5) Determination of the source offset perpendicular to the slew.
6) Source fitting with 2-dimensional gaussian with fixed slew offset.
7) Empirical flux correction for signal loss due to the fast crossing of the sources during slews.

Item 7 is derived from the ratios of uncorrected Serendipity Survey fluxes (steps 1 – 6) with those of models or raster map photometry (Figure 6). Brighter sources suggest a ratio of 0.6 . For fainter sources there is a somewhat higher scatter around higher values.

The achieved photometric accuracy is $<$ 40 %. The positional accuracy of the first catalogue (Stickel et al. 2000) is $< 45''$.

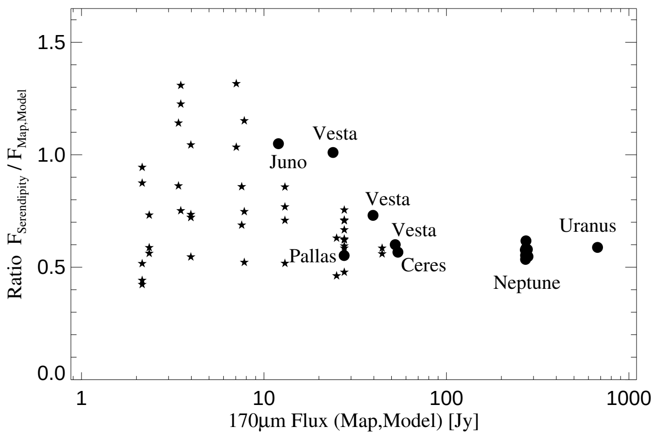

Figure 6. Comparison of fluxes derived for sources with both Serendipity Survey detections and staring raster map or model fluxes. Data points along a vertical line belong to the same source which was detected several times by the Serendipity Survey, but at different distances from the slew path. The ratio of $F_{\mathrm{Serendipity}}$ *and* $F_{\mathrm{Map,Model}}$ *is a measure of the empirical flux correction to be applied to Serendipity Survey fluxes in order to account for signal losses due to the fast crossing of sources during the slews. Beside planets and asteroids, mainly galaxies are used to establish this relation.*

8.8. Calibration Accuracy Overview

Table 12 shows that meanwhile very good accuracy numbers are achieved for most detectors over a wide flux range with the automatically generated data products. For the faint flux level, where the accuracy is limited by the signal-to-noise ratio, satisfying numbers are achieved, if an optimum observing mode provided highest contrast and redundancy.

8.9. Scientific Validation Status

Table 13 gives the validation status of all 28 ISOPHOT observation submodes. It shows that a high completion both in the number of submodes and in the total number of executed astronomical observations could be achieved. The ISO Post Operations Phase with the coordinated activities of three data centres was necessary to consolidate the quality of the ISOPHOT data products. The main open issues are photometry in non-standard apertures with PHT-P and point source photometry from chopped oversampled maps.

9. Outlook for Active Archive Phase

The ISOPHOT Data Centre will continue to improve the general calibration and the quality of specific products during the upcoming five year period of the ISO Active Archive Phase. The activities will comprise:

- Refinement of the current calibration files, like time and orbit-phase-dependent dark signals and default responsivities.
- Introduction of new calibration items, like the contribution of by-passing sky light to the FCS signals (for all observations which do not contain a cold FCS measurement).
- Scientific assessment of photometry in non-standard apertures and establishment of correction factors with regard to the standard apertures.
- Tests of signal transient corrections (interactive and automatic).
- Bulk processing of data sets with improved calibration or for easier access of photometric information (e.g. background subtracted source fluxes for mini-map, nodding and sparse map observations) and import into the Archive.
- Production of homogeneously processed catalogues, like Serendipity Survey point and extended source catalogues, photometric sky background data base or PHT-S spectral atlas.
- Product quality and validation checks.

10. Conclusions

From the previous sections the following résumé can be drawn:

- Ground calibration programs proved to be essential to establish the in-orbit calibration guide-lines (IOCRD) and to influence the AOT and operations design.
- The pre-flight determination of operational detector parameters (bias voltage, temperatures, curing sequences) worked successfully and facilitated the task of the instrument inflight commissioning.
- Spacecraft orbits crossing the radiation belts need a sufficiently long timeline to account for temporal variations in order to optimise the length of the science windows. More flexible mission planning should allow to schedule sensitive measurements on clean parts of the revolution.
- Probing the sensitivity limits of an instrument in the FIR requires a comprehensive program to test the optimum observation strategy on a number of faint standard sources.
- The calibration source data base should be large enough to cover practically the whole flux range of an instrument to cope with possible non-linearities.
- Reviews of the calibration status during the mission help to identify deficits. Statistics of the instrument configurations determines the key set-ups.
- Both calibration approaches, namely (1) the characterisation and correction for individual instrumental effects (PHT–P, PHT–C) and (2) the integral correction having the same measurement procedure for the unknown source as for the celestial standard (PHT–S) led to good calibration accuracies. Approach 2 appears to be slightly favourable, but allows less flexibility in measurement configurations.
- A high completeness of the scientific validation of the 28 different ISOPHOT submodes could be achieved by the end of the ISO Post Operations Phase.
- A pre-requisite for the achievements were the coordinated efforts of the three data centres at MPIA Heidelberg (PHTNDC), Villafranca (IDC) and RAL (UKIDC) bringing in the expertise in calibration, algorithmic development and

Table 12. ISOPHOT Photometric Calibration Accuracy Overview.

detector	source type point / extended	source brightness	typical on-source integration [s]	absolute accuracy [%]	reproducibility 1 σ of 20 samples [%]	multi-filter accuracy [%]
P1	p, star	50 – 6000 Jy	32	$<$10	5	$<$20
P1	p, star	0.1 – 50 Jy	$\leq$256	40	10	–
P1	p, chop	0.06 – 10 Jy	128	$<$30	$<$15	–
P2	p, star	10 – 200 Jy	32	$<$10	2	5
P2	p, star	0.5 – 10 Jy	$\leq$256	$<$15	12	–
P2	p, chop	0.2 – 20 Jy	128	$<$30	$<$10	–
P3	p, star	0.5 – 25 Jy	32	10	7	$<$10
P3	p, star	$<$0.5 Jy	$\leq$256	20	7	–
P3	p, chop	$\geq$1 Jy**	128	$<$30	$<$10	–
C100	p, star	0.5 – 25 Jy	32	15	$\geq$3	$<$25
C100	p, star	0.05 – 0.5 Jy	$\leq$256	$<$25*	20	–
C100	e, star	5 – 15 MJy sr^{-1}	32	25	10	20
C100	p, chop	$\geq$1 Jy**	128	$<$30	$<$15	–
C200	p, star	1 – 900 Jy	128	10	10	20
C200	p, star	0.2 – 1 Jy	$\leq$256	$<$20*	10	–
C200	e, star	4 – 10 MJy sr^{-1}	64	20	6	20
C200	p, chop	$\geq$2 Jy**	128	$<$40	–	–
SS	p, star	1 – 6000 Jy	256	$<$10	–	$<$15
SS	p, chop	0.5 – 500 Jy	1024	$<$10	–	$<$10
SS	e, star	30 – 3000 MJy sr^{-1}	256	$<$10	–	$<$15
SL	p, star	0.3 – 1500 Jy	256	$<$10	–	$<$15
SL	p, chop	0.2 – 200 Jy	1024	$<$10	–	$<$10
SL	e, star	5 – 10000 MJy sr^{-1}	256	$<$10	–	$<$15

* for mini-map photometry using PCAS products
** for fainter fluxes careful estimate of cirrus confusion necessary

scientific validation. Sufficient time and manpower has to be allocated to achieve a certain data quality. The too early releases of data products were not helpful, even if they are labelled as preliminary.

Finally we would like to comment on the initial calibration philosophy:

- Due to the limited lifetime of ISO, there was the requirement on the IDTs to plan the full Performance Verification Phase (for PHT these were 16 revolutions with about 1000 observations) in every detail. Because of the various small launch delays this meant to plan the PV Phase three times with varying calibration targets due to visibility constraints. This planning effort allocated nearly all calibration expert manpower pre-flight so that issues of the data reduction received less attention. For the future it should be considered whether detailed pre-planning is a gain, if the tools to judge the instrument performance and data quality are less well developed and some mission time passes before counter-measures in the form of adjustments to, or even re-design of, observing modes or calibration strategies can be taken. A more balanced approach appears to be preferable, in particular, since all IDTs demonstrated in the PV Phase that fast re-planning of a full revolution within 4 days worked successfully.
- The compactness of the PV Phase made it necessary to allocate most of the calibration manpower on planning and most of the data analysis had to be restricted to preliminary checks. Although the learning was tremendous during this phase and was fed back as much as possible into improved observation design, a more staggered PV Phase with consolidation of intermediate results and a staggered release of observing modes would have been a better approach. This is demonstrated e.g. by the late release of optimised polarisation modes only after detailed understanding of their performance. In addition more manpower would have allowed to perform several important calibration analysis work packages in parallel.
- The conditions of the PV Phase were not one-to-one equivalent to those of the Routine Phase, since the one-instrument operation resulted in different temperature levels of the Optical Support Structure and hence non-temperature stabilised detectors showed different transient behaviour.
- The time allocated to calibration in the Routine Phase was 1 out of 7 revolutions. The calibration time was fairly equally split among the four instruments, so that 4.1 hours per week or a total equivalent of 28.3 revolutions out of 797, i.e. 3.6%, was available for ISOPHOT calibration. In order to achieve a coherent calibration, the PIDT had to request time for several engineering and deficit programmes. This is an

Table 13. Scientific Validation of ISOPHOT OLP AOT Processing for the ISO Legacy Archive. The 11 AOTs have been divided into 28 submodes and the respective number of executed astronomical observations is given. An observation in multi-filter and multi-aperture mode can comprise several measurements. The sparse map modules have been counted individually. OLP Versions 5 and 6 were released during the ISO mission, OLP Version 7 is the end-of-mission pipeline, OLP Versions 8 and 9 were released during Post Operations Phase and OLP version 10 is the Legacy Archive Version. "No" means that the submode is still unvalidated in the Legacy Archive due to low priority or on-going calibration work and will be validated later during the Active Archive Phase.

AOT	observation type	submode	# of AOs	scientific validation with	comments
PHT03 (P)	multi-	staring point source	961	V6	for standard apertures
	filter	staring ext. source	270	no	
	photometry	nodding	230	V6	for standard apertures
		chopped	1134	V10	
		raster map	431	no	
PHT04 (P)	multi-	staring point source	219	V10	relative curve of growth
	aperture	staring ext. source	36	V10	for extent < 2 arcmin
	photometry	chopped	17	no	sequ: ≥ 4 aper. (120,180)
PHT05 (P)	absolute	staring point source	57	V6	for standard apertures
	photometry	staring ext. source	162	no	
PHT17 (P)	sparse map	staring point source	682	V6	for standard apertures
18 , 19	photometry	staring ext. source	524	no	
PHT22 (C)	multi-	staring point source	373	V7	
	filter	staring ext. source	123	V7	
	photometry	nodding	29	V7	
		chopped	1887	V10	limited by sky confusion
		raster map	2884	V8.4	ff quality for > 20 RP
PHT25 (C)	absolute	staring point source	54	V7	
	photometry	staring ext. source	149	V7	
PHT32 (C)	oversampled	chopped mapping	1565	V10	partially validated w.r.t.
	mapping				SB, ff quality
PHT37 (C)	sparse map	staring point source	2109	V7	
38 , 39	photometry	staring ext. source	710	V7	
PHT40 (S)	spectroscopy	staring point source	835	V5	
		staring ext. source	102	V6	
		chopped	412	V6	
		raster map	135	V6	
PHT50 (P)	aperture	staring point &	15	V7	interactive processing
	polarimetry	ext. source			& special FORTRAN routine
PHT51 (C)	array	staring point &	110	V7	interactive processing
	polarimetry	ext. source			& special FORTRAN routine
		raster		V7	beam effects for ext. sources?

indicator that more routine calibration time should have been allocated for PHT.

ACKNOWLEDGEMENTS

We acknowledge contributions to the ISOPHOT calibration by the members of the ISOPHOT Instrument Dedicated Team, the ISOPHOT consortium, the ISOPHOT Data Centre in Heidelberg, the ISO Data Centre in Villafranca and the UK ISO Data Centre at RAL. This work was supported by the Max-Planck Society and funds from the DLR (formerly DARA), Bonn. The ISOPHOT Data Centre at MPIA is supported by Deutsches Zentrum für Luft- und Raumfahrt e.V. (DLR) with funds of Bundesministerium für Bildung und Forschung, grant no. 50 QI 9801 3. The authors take sole responsibility for this report.

REFERENCES

Ábrahám, P., Acosta-Pulido, J.A., Klaas, U. et al., 2003, this volume

Acosta-Pulido, J.A. & Ábrahám, P., 2003, this volume

Burgdorf, M. & Orton, G.S., 2003, this volume

Cohen, M., 2003, this volume

del Burgo, C., Ábrahám, P., Klaas, U. and Héraudeau, P., 2003, this volume

Gabriel, C., 2003, this volume

Hacking, P. & Houck, J.R., 1987, ApJ Suppl. 63, 311

Hammersley, P., 2003, this volume

Héraudeau, P., Ábrahám, P., Klaas, U., Kiss, C. and del Burgo, C., 2003, this volume

Kiss, Cs., Ábrahám, P., Klaas, U., Juvela, M., Lemke, D., 2001, A&A, 379, 1161

Klaas, U., Laureijs, R.J., Müller T.G., Kreysa, E. and Krätschmer W., 1999, Proceedings of the Workshop "ISO Polarisation Observations", (Eds.) R.J. Laureijs & R. Siebenmorgen, ESA SP-435, 19

Laureijs, R.J. & Klaas, U., 1999, Proceedings of the Workshop "ISO Polarisation Observations", (Eds.) R.J. Laureijs & R. Siebenmorgen, ESA SP-435, 27
Laureijs, R.J & Levine, D. (eds.), 1997, "Taking ISO to the Limits: Exploring the faintest sources in the infrared", Proceedings of a workshop, Feb. 1997
Lemke, D., Grözinger, U., Schulz B. et al., 2003a, this volume
Lemke, D., Kranz, T., Klaas U. et al., 2003b, this volume
Lemke, D., Klaas, U., Abolins J. et al., 1996, A&A 315, L64
Müller, T.G. & Lagerros, J.S.V., 2003, this volume
Richards, P.J., Klaas, U., Laureijs R.J. et al., 2003, this volume
Schulz, B., 2003, this volume
Stickel, M., Lemke, D., Klaas, U. et al., 2000, A&A 359, 865
Tuffs, R., Gabriel, C., 2002, In: Proceedings of the "ISOPHOT Workshop on P32 Oversampled Mapping", (Eds.) B. Schulz, N. Lu, S. B. Peschke, ESA SP-482
Wilke, K., Grözinger, U., Klaas, U. and Lemke D., 2003, this volume